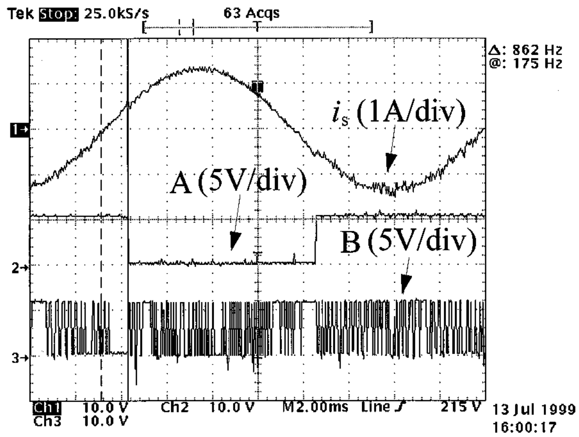

(a)

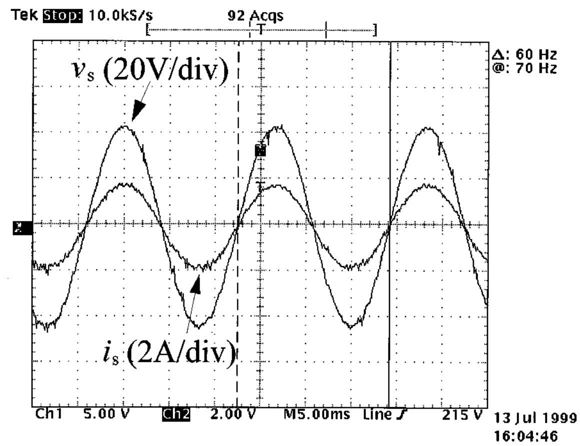

(b)

Fig. 3. (a) Waveforms of I_s, A, and B. (b)Waveforms of v_s and I_s.

When the upper band of the second comparator is exceeded (A is low), the switching patterns are changed to force i_s to remain in the inner loop again. Fig. 3(b) shows the waveforms of v_s and i_s. The input power factor is nearly unity.

V. Conclusions

This letter has presented a hysteresis current controller with two loops for a four-switch boost rectifier to operate under the phase-adjusted PWM scheme. The inner loop confines the input current ripple within a smaller hysteresis band. The outer loop determines the instants to change the switching patterns. Experimental results has been recorded to verify the effectiveness of the proposed controller. The discussed system is specially suitable and cost-worthy for high-power applications.

References

[1] J. C. Salmon, "Circuit topologies for single-phase voltage-doubler boost rectifiers," *IEEE Trans. Power Electron.*, vol. 8, pp. 521–529, Oct. 1993.

[2] ——, "Techniques for minimizing the input current distortion of current-controlled single-phase boost rectifiers," *IEEE Trans. Power Electron.*, vol. 8, pp. 509–520, Oct. 1993.

[3] Y.-K. Lo and N.-C. Lai, "On evaluating the input current distortion with current slopes for single-phase switch-mode rectifiers," in *Proc. IEEE ISIE'98*, 1998, pp. 77–80.

On Speed and Rotor Position Estimation in Permanent-Magnet AC Drives

J. Solsona, M. I. Valla, and C. Muravchik

***Abstract*—This letter deals with rotor position and speed estimation of permanent magnet ac drives. Two reduced-order observers, a linear (AO) and a nonlinear one (NLO), are compared. An adaptive speed estimation scheme is also considered. Analysis and simulations show that the NLO has better performance and demands less computational load than the AO plus the adaptive scheme.**

***Index Terms*—Observers, state estimation, synchronous motor drives.**

I. Introduction

Rotor position and speed of permanent-magnet synchronous motors (PMSMs) may be estimated with observers based upon measurements of the electrical variables of the motor. Different approaches to estimate the state variables can be found in the literature. In [1] and [2], nonlinear full-order observers are employed for speed estimation. The rotor position is obtained integrating the speed estimate in open loop. In [3], an algorithm to estimate flux and current by the integration of differential equations was proposed. In [4], an open-loop model of the motor back electromotive force (EMF) is assumed under electrical steady-state operation. In [5] and [6], the implementation of an extended Kalman filter (EKF) is proposed for speed and rotor position estimation.

An alternative approach is to use reduced-order observers to decrease the computational load. Among them, reduced-order Luenberger observers can be found in their linear and nonlinear versions. Versions that result in linear Luenberger observers (AOs) can be found in [7] and [8], whereas a nonlinear solution (NLO) was proposed in [9]. In these approaches, the EMF is estimated first and then rotor position and speed are reconstructed using the relationship between EMF and rotor variables. In order to obtain good estimates, the EMF must be estimated with low error since the EMF estimation error is propagated to rotor variables. In [7] and [8], the proposed observers use approximate equations for estimating EMF. Due to this approximation, an EMF residual error is propagated to the estimated rotor position and speed. This error depends on the rotor speed and acceleration of the motor. The authors of [7] proposed to overcome the limitations of the AO with an adaptive scheme to estimate the rotor speed. This scheme reduces the estimation error, adding complexity to the estimation algorithm. The EMF residual error can be completely avoided using the nonlinear reduced order Luenberger observer proposed in [9].

Manuscript received June 23, 1999; revised May 27, 2000. Abstract published on the Internet July 1, 2000. This work was supported by the National University of La Plata (UNLP), National University of Comahue, Agency for the Promotion of Science and Technology (ANPCYT), National Research Council (CONICET), and Buenos Aires Province Research Council (CICPBA).

J. Solsona is with the National Research Council (CONICET) and also with the Automatic Control and Systems Group, Electrical Engineering Department, National University of Comahue, Buenos Aires 1400, Argentina (e-mail: jsolsona@uncoma.edu.ar).

M. I. Valla is with the Laboratory of Industrial Electronics, Control and Instrumentation, Electrical Engineering Department, National University of La Plata, 1900 La Plata, Argentina, and also with the National Research Council (CONICET).

C. Muravchik is with the Laboratory of Industrial Electronics, Control and Instrumentation, Electrical Engineering Department, National University of La Plata, 1900 La Plata, Argentina, and also with the Buenos Aires Province Research Council (CICPBA).

Publisher Item Identifier S 0278-0046(00)08850-X.

In this letter, we compare the AO, with and without adaptive speed estimation, with the NLO. We describe both observers, and present the equations required for the observers implementation. We evaluate the performance of the observers through simulations and, finally, draw some conclusions.

II. Position and Speed Estimation via EMF

A. Configuration of the Observers

The motor is described in a stationary two-axes reference frame, and the mechanical variables are converted to electrical angles. The machine model can be written as follows:

$$\dot{\theta}_{re} = \omega_{re} \tag{1}$$

$$\dot{\omega}_{re} = \frac{K_T}{J}[-i_\alpha \sin(\theta_{re}) + i_\beta \cos(\theta_{re})] - \frac{B}{J}\omega_{re} \tag{2}$$

$$\dot{i}_\alpha = \frac{-R}{L} i_\alpha + \frac{K_E}{L}\omega_{re} \sin(\theta_{re}) + \frac{v_\alpha}{L} \tag{3}$$

$$\dot{i}_\beta = \frac{-R}{L} i_\beta - \frac{K_E}{L}\omega_{re} \cos(\theta_{re}) + \frac{v_\beta}{L} \tag{4}$$

where i_α, i_β and v_α, v_β are currents and voltages in the stationary two-axes reference frame. The electrical parameters R, L, and K_E are resistance, inductance, and EMF constant, respectively. The mechanical variables and parameters θ_{re}, ω_{re}, B, J, and K_T are rotor position, rotor speed, viscosity, inertia, and torque constant, respectively.

Taking into account the motor electrical equations (3) and (4), it is clear that the rotor position and speed information is contained in the back-EMF terms, given by

$$e_\alpha = -K_E\omega_{re} \sin(\theta_{re}) \tag{5}$$

$$e_\beta = K_E\omega_{re} \cos(\theta_{re}). \tag{6}$$

The observers under consideration differ in the way they estimate the back-EMF terms. The AO considers slowly varying approximations of e_α and e_β, and the EMF estimations are built with zero dynamic part and driven by the correction terms

$$\dot{\hat{e}}_{\alpha_{AO}} = Lg_{11}(\dot{\hat{i}}_\alpha - \dot{i}_\alpha) + Lg_{12}(\dot{\hat{i}}_\beta - \dot{i}_\beta) \tag{7}$$

$$\dot{\hat{e}}_{\beta_{AO}} = Lg_{21}(\dot{\hat{i}}_\alpha - \dot{i}_\alpha) + Lg_{22}(\dot{\hat{i}}_\beta - \dot{i}_\beta) \tag{8}$$

where the gains g_{ij} are calculated using a pole-assigment technique of linear observers [7]. The NLO obtains the dynamic equations for the EMF calculating the time derivatives of (5) and (6), and adding the correction terms

$$\dot{\hat{e}}_\alpha = -K_E\left[\dot{\hat{\omega}}_{re}\sin(\hat{\theta}_{re}) + \hat{\omega}_{re}^2\cos(\hat{\theta}_{re})\right] + Lg_{11}(\dot{\hat{i}}_\alpha - \dot{i}_\alpha) + Lg_{12}(\dot{\hat{i}}_\beta - \dot{i}_\beta) \tag{9}$$

$$\dot{\hat{e}}_\beta = K_E\left[\dot{\hat{\omega}}_{re}\cos(\hat{\theta}_{re}) - \hat{\omega}_{re}^2\sin(\hat{\theta}_{re})\right] + Lg_{21}(\dot{\hat{i}}_\alpha - \dot{i}_\alpha) + Lg_{22}(\dot{\hat{i}}_\beta - \dot{i}_\beta) \tag{10}$$

where $\dot{\hat{\omega}}_{re}$, $\dot{\hat{i}}_\alpha$, and $\dot{\hat{i}}_\beta$ are calculated with (2)–(4) evaluated on the estimated values. The gains g_{ij} are selected to set the convergence speed in a way similar to pole assignment in linear systems [9].

The rotor position and speed can be reconstructed from EMF estimated values as follows:

$$\hat{\theta}_{re} = tg^{-1}\left(\frac{-\hat{e}_\alpha}{\hat{e}_\beta}\right) \tag{11}$$

$$\hat{\omega}_{re} = \frac{1}{K_E}\sqrt{\hat{e}_\alpha^2 + \hat{e}_\beta^2} \tag{12}$$

where $\hat{e}_\alpha$ and $\hat{e}_\beta$ are replaced by $\hat{e}_{\alpha_{AO}}$ and $\hat{e}_{\beta_{AO}}$ for the AO.

B. Estimation Errors Using AO

NLO and AO significantly differ regarding the estimation errors of the EMF and, consequently, those of speed and rotor position. The NLO is an asymptotic state estimator of the EMF as it was demonstrated in [9]. Therefore, assuming the parameters are perfectly known, position and speed estimated as in (11) and (12) converge to the actual values. On the other hand, the AO presents estimation errors due to the approximations made for the EMF terms, even when all the parameters are accurately known. In [10], we carried out an extensive analysis of the EMF estimation errors, and their propagation to the rotor position and speed calculations. The errors depends on the actual speed and acceleration of the motor. First, we considered the most favorable case for the AO, that is, the motor running at constant speed. In this case, the steady-state errors result in

$$\varepsilon_{\omega_{re}}(\infty) = \Omega_{re}\left(-1 + \frac{g}{\sqrt{g^2 + \Omega_{re}^2}}\right) \tag{13}$$

$$\varepsilon_{\theta_{re}}(\infty) = \tan^{-1}\left(\frac{-\Omega_{re}}{g}\right). \tag{14}$$

Equations (13) and (14) show that the AO has steady-state errors which depend on the observer gain and the running speed of the motor. To reduce the errors, the observer gain should be much larger than Ω_{re}, and this is not easy to achieve at medium and high speeds. Moreover, this gain multiplies the current derivatives, so increasing it makes the observer very sensitive to the current ripple and noise. In [10], we also investigated the effect of parameters deviations in both observers. We concluded that they have similar sensitivity to variations in R. The AO is more sensitive than the NLO when variations in L are considered. The NLO presents small errors due to uncertainties in K_E, B and J, while the AO is insensitive to these parameters. In every case, the errors of the NLO are well below those of the AO.

C. Implementation of the Different Observers

To avoid taking derivatives of the measurements, the following equations are actually implemented for the NLO (see [9]), where the actual rotor position and speed are calculated instead of those in electrical degrees:

$$\dot{\nu}_1 = \frac{p^2K_T\hat{e}_\alpha}{JK_E\hat{\omega}^2}(i_\alpha\hat{e}_\alpha + i_\beta\hat{e}_\beta) - \frac{B}{J}\hat{e}_\alpha - \frac{\hat{e}_\beta\hat{\omega}}{p} + g(-Ri_\alpha - \hat{e}_\alpha + v_\alpha) \tag{15}$$

$$\dot{\nu}_2 = \frac{p^2K_T\hat{e}_\beta}{JK_E\hat{\omega}^2}(i_\alpha\hat{e}_\alpha + i_\beta\hat{e}_\beta) - \frac{B}{J}\hat{e}_\beta + \frac{\hat{e}_\alpha\hat{\omega}}{p} + g(-Ri_\beta - \hat{e}_\beta + v_\beta) \tag{16}$$

$$\hat{e}_\alpha = \nu_1 - Lgi_\alpha \tag{17}$$

$$\hat{e}_\beta = \nu_2 - Lgi_\beta \tag{18}$$

$$\hat{\omega} = \frac{\sqrt{\hat{e}_\alpha^2 + \hat{e}_\beta^2}}{pK_E} \tag{19}$$

$$\hat{\theta} = \frac{1}{p}tg^{-1}\left(\frac{-\hat{e}_\alpha}{\hat{e}_\beta}\right) \tag{20}$$

where p is the number of pole pairs of the motor. Similarly, the AO is implemented with

$$\dot{\xi}_1 = g(-Ri_\alpha - \hat{e}_{\alpha_{AO}} + v_\alpha) \tag{21}$$

$$\dot{\xi}_2 = g(-Ri_\beta - \hat{e}_{\beta_{AO}} + v_\beta) \tag{22}$$

$$\hat{e}_{\alpha_{AO}} = \xi_1 - Lgi_\alpha \tag{23}$$

$$\hat{e}_{\beta_{AO}} = \xi_2 - Lgi_\beta \tag{24}$$

$$\hat{\omega}_{AO} = \frac{\sqrt{\hat{e}_{\alpha_{AO}}^2 + \hat{e}_{\beta_{AO}}^2}}{pK_E} \tag{25}$$

$$\hat{\theta}_{AO} = \frac{1}{p}tg^{-1}\left(\frac{-\hat{e}_{\alpha_{AO}}}{\hat{e}_{\beta_{AO}}}\right). \tag{26}$$

In [7], the authors proposed a model reference adaptive system (MRAS) for estimating the EMF nonlinear terms. In this way, they

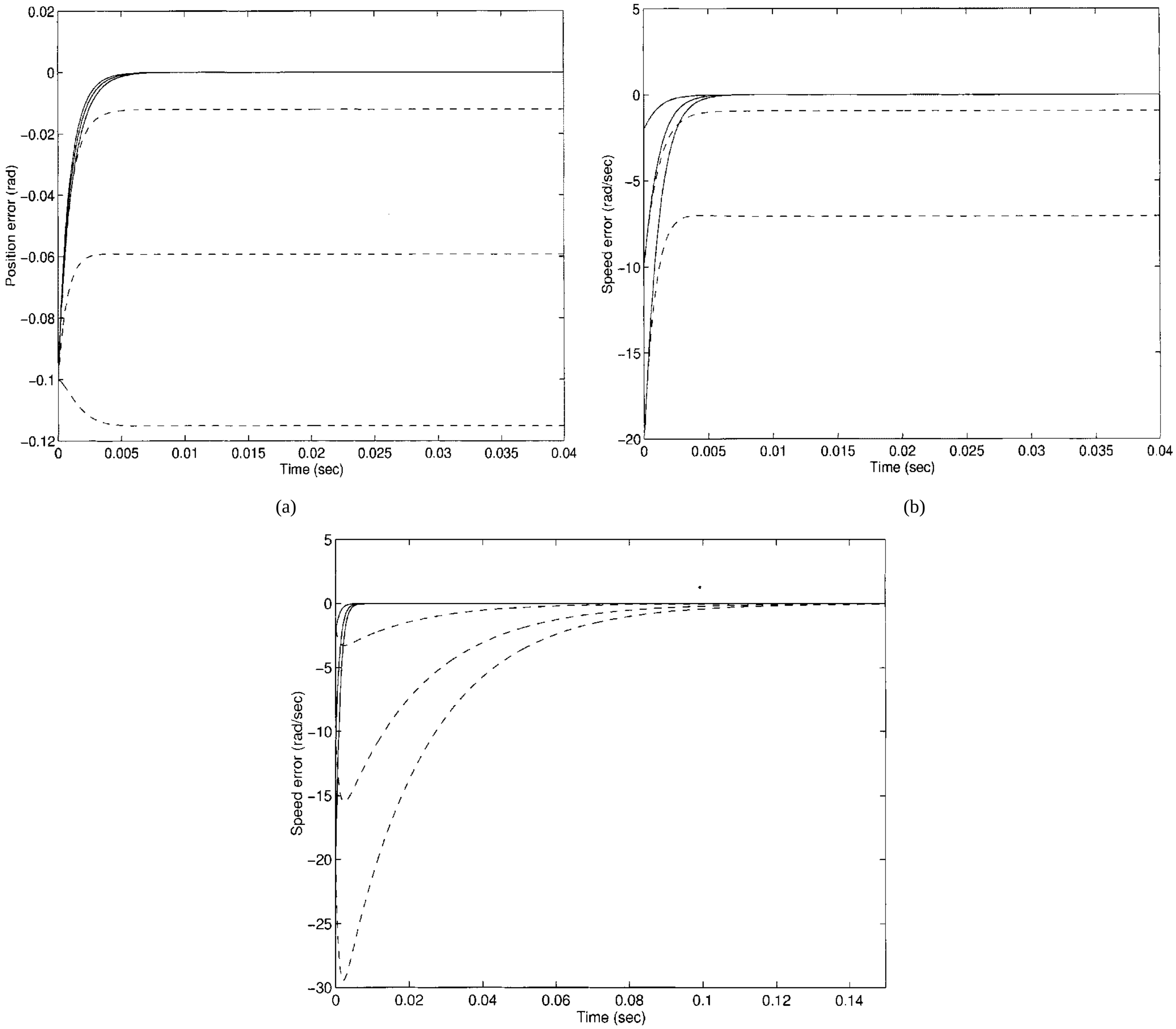

Fig. 1. Estimation errors for the motor running at constant speed. (a) Rotor position error: NLO (solid line) and AO (dashed line). (b) Speed error: NLO (solid line) and AO (dashed line). (c) Speed error: NLO (solid line) and MRAS (dashed line).

achieve a decrease in the speed estimation error. Nevertheless, it must be remarked that only a part of the nonlinear terms is considered and that the observer correction term is calculated via Popov's hyperstability theory assuming constant speed. For these reasons, a large error may appear when a variable speed profile has to be tracked. The equations to be implemented are (see [7])

$$\dot{\tilde{e}}_\alpha = -\hat{\omega}_{Ad}\tilde{e}_\beta + \frac{\hat{\omega}_{AO}}{c_3}(\hat{e}_{\alpha_{AO}} - \tilde{e}_\alpha) \tag{27}$$

$$\dot{\tilde{e}}_\beta = \hat{\omega}_{Ad}\tilde{e}_\alpha + \frac{\hat{\omega}_{AO}}{c_3}(\hat{e}_{\beta_{AO}} - \tilde{e}_\beta) \tag{28}$$

$$\hat{\omega}_{Ad} = \frac{c_1}{\hat{\omega}_{AO}}[(\hat{e}_{\beta_{AO}} - \tilde{e}_\beta)\tilde{e}_\alpha - (\hat{e}_{\alpha_{AO}} - \tilde{e}_\alpha)\tilde{e}_\beta] + \frac{c_2}{\hat{\omega}_{AO}} \cdot \int_0^t [(\hat{e}_{\beta_{AO}} - \tilde{e}_\beta)\tilde{e}_\alpha - (\hat{e}_{\alpha_{AO}} - \tilde{e}_\alpha)\tilde{e}_\beta]\,dt \tag{29}$$

where c_1, c_2, and c_3 are constants to be designed.

The speed error obtained with this algorithm for constant speed is smaller than the error obtained with the AO. Nevertheless, it must be remarked that the speed error strongly depends on the motor acceleration.

It must be pointed out that, while NLO converges exponentially, the adaptive velocity algorithm convergence is not guaranteed. In addition, regarding the computational burden, the NLO is much simpler than the algorithm given by (21)–(29). In the AO, the complex equations (15) and (16), are approximated by the simpler ones (21) and (22). However, the adaptive scheme introduced to overcome the limitations of the AO adds up three nonlinear equations (27)–(29), which makes it more complex than the NLO.

III. Comparison Through Simulations

A model of the permanent-magnet ac drive (PMACD), which replicates the parameters and operating conditions described in [7], is built and simulated. Each observer measures voltages and currents of this model and performs the estimations open loop. The rotor position and speed errors are built comparing the estimated values of the observers

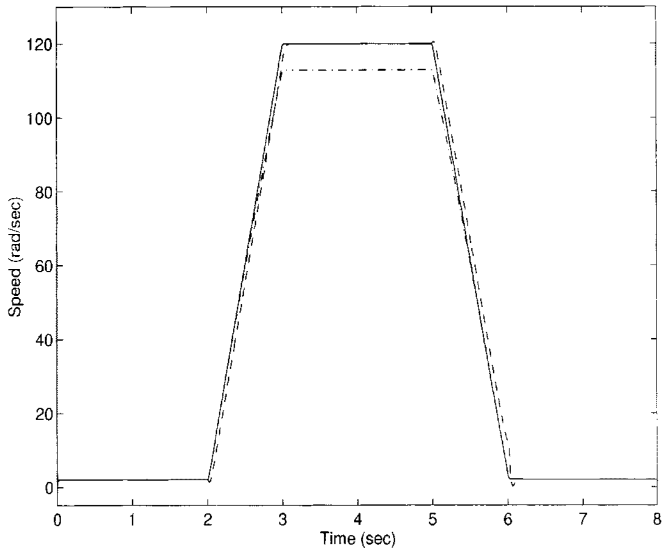

(a)

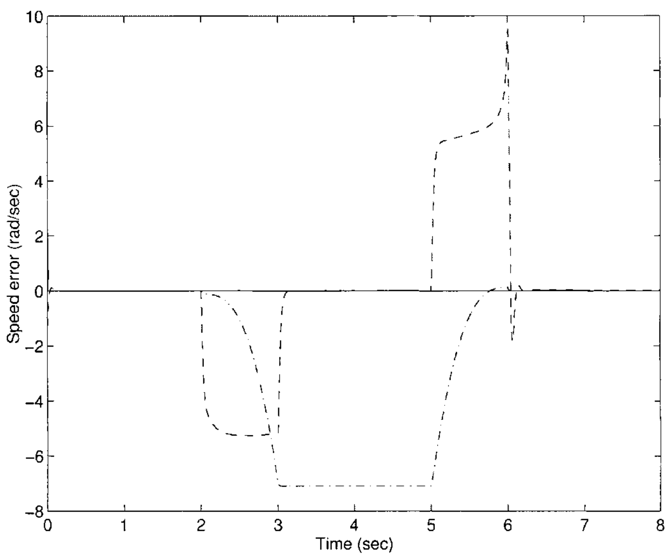

(b)

Fig. 2. Observers performance for varying speed. (a) Rotor speed: actual motor (solid line), NLO (dotted line), MRAS (dashed line), and AO (dashed–dotted line). (b) Speed error: NLO (solid line), MRAS (dashed line), and AO (dashed–dotted line).

against the rotor position and speed of the simulated drive. The data and parameters of the motor are $P_N = 1.2$ kW, $\Omega_N = 1200$ r/min, pole pairs = 3, $L = 13.4$ mH, $R = 1.6\ \Omega$, $K_E = 0.288$ V·s/rad, $K_T = 11.3$ kg·cm/A, $J = 0.434$ kg·cm·s^2, and $B = 0.0434$ kg·s/rad. A gain g equal to 1000 is used for both AO and NLO. The gains of the adaptive speed estimator coincide with those given in [7]. For this reason, the constants c_1, c_2, and c_3 are 0.0347, 5208, and 0.1, respectively.

We consider a test when the motor runs at constant speed and the observers are started with several initial conditions. Fig. 1 shows the transient behavior of the AO, the NLO, and the MRAS estimators for the motor running at nominal speed (120 rad/s), medium speed (60 rad/s), and low speed (12 rad/s). Fig. 1(a) shows the rotor position error for the AO and the NLO observers. It is seen that both observers present an exponential transient, but while the NLO converges to zero error in every case, the AO converges to a steady-state error which depends on the running speed as predicted by (14). Fig. 1(b) shows the corresponding speed errors. The same comments of Fig. 1(a) apply here,

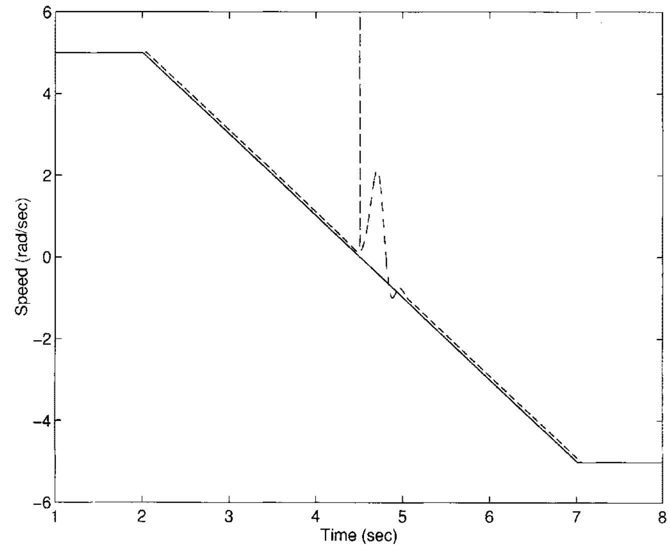

Fig. 3. Observers performance with reversal speed profile. Actual speed (solid line), NLO (dotted line), MRAS (dashed line), and AO (dashed–dotted line).

and the steady-state errors match those predicted by (13). In Fig. 1(c), the adaptive speed estimates are compared with those of the NLO. It is clearly seen that the convergence of the adaptive speed estimator is much slower than the NLO (and the AO). Both estimates converge to zero error while the running speed is kept constant. This is an improvement of the adaptive scheme with respect to the AO regarding the steady-state performance.

A reference speed profile is applied to the drive. The motor is accelerated from 3 to 120 rad/s (nominal speed) and then decelerated to 3 rad/s. Fig. 2(a) depicts the actual and estimated speeds. The NLO estimate is indistinguishable from the actual speed, the MRAS estimate presents an error during acceleration and braking, and the AO has a noticeable error at high speeds. This is better illustrated in Fig. 2(b), where the speed errors for the three approximations are shown. It is seen that the estimates of the NLO are not affected by the transient in the motor speed. In the AO, the speed error increases with the running speed, and is slightly affected by the motor acceleration. The adaptive estimation has a better convergence at constant speed but it presents high errors during acceleration. It also presents some oscillations during motor braking when the rotor speed approaches zero speed, which represents a clear risk of instability of the algorithm.

A speed reversal test is performed with the three observers. For a test similar to that in Fig. 2, but continued to negative nominal speed, it is observed that the MRAS scheme is unstable while there is no particular problem with the other two. A low-acceleration test is also carried on with the motor running at 5 rad/s and reversed to -5 rad/s in 5-s time, as shown in Fig. 3. It is clearly seen that there is no problem for the AO and the NLO to follow this speed profile. Their estimates are indistinguishable from the actual speed. However, the adaptive scheme shows some difficulties for tracking the speed reversal even with a low acceleration rate. From (29), it is clear that any difference between both EMF estimates when $\hat{\omega}_{AO}$ tends to zero will result in a very high value of the estimated speed, as shown by the trace line in Fig. 3.

It is important to remark that, in the tests as presented above, the NLO and the AO have no problem starting from standstill with any value of acceleration. Also, the startup for the MRAS is not difficult, since it is possible to perturb the zero initial value to a $\hat{\omega}_{\mathrm{AO}}$ slightly different from zero.

Finally, we show the impact of unmodeled space harmonics of EMF. We considered a trapezoidal EMF distribution which results in 4.2% of the fifth and 2.5% of the seventh harmonics to be present in the actual distribution of the EMF of the motor, but not modeled in

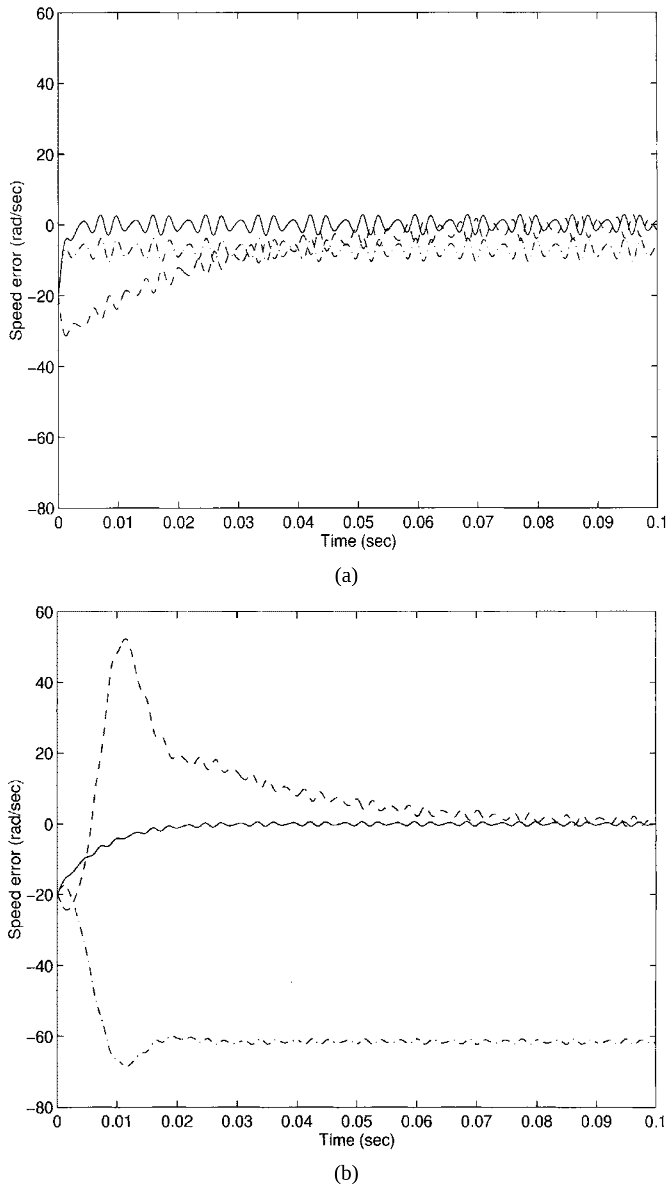

Fig. 4. Estimation errors considering unmodeled space harmonics of EMF. (a) $g = 1000$: NLO (solid line), MRAS (dashed line), and AO (dashed–dotted line). (b) $g = 200$: NLO (solid line), MRAS (dashed line), and AO (dashed–dotted line).

the observers. The results of this test for nominal speed are shown in Fig. 4(a). It is clearly seen that, for the three observers, the unmodeled space harmonics appear as ripple in the speed estimates. This effect can be reduced by decreasing the observer's gain g_{ij} as shown in Fig. 4(b), where $g = 200$ is considered. We notice here that the ripple is much smaller in all three estimates. Moreover, the NLO observer only presents a slower convergence, while the AO shows a much larger steady-state error, and the MRAS scheme presents a highly demanding transient.

IV. Conclusions

Different algorithms for estimating rotor position and speed of a PMSM were compared. The AO reduced-order linear observer of [7] and [8], the MRAS speed estimation proposed in [7], and the NLO nonlinear Luenberger observer of [9] were considered. The methods were compared on the basis of their estimation errors when the motor runs at constant and varying speed.

After the complete set of analysis and simulations, we conclude that the AO presents steady-state errors which depend on the running speed. The MRAS speed estimation scheme decreases these steady-state errors, but it shows large errors during acceleration, and there is also some risk of instability in the estimation. The NLO presents a much better overall performance, even when parameters uncertainties are considered. The NLO implementation would require a higher computational complexity than that of the AO, but smaller than needed by the MRAS speed estimation.

References

[1] L. Jones and J. Lang, "A state observer for the permanent-magnet synchronous motor," *IEEE Trans. Ind. Electron.*, vol. 36, pp. 374–382, Aug. 1989.

[2] T. Low, T. Lee, and K. Chang, "A nonlinear speed observer for permanent-magnet synchronous motor," *IEEE Trans. Ind. Electron.*, vol. 40, pp. 307–315, June 1993.

[3] N. Ertugrul and P. Acarnley, "A new algorithm for sensorless operation of permanent magnet motors," *IEEE Trans. Ind. Applicat.*, vol. 30, pp. 126–133, Jan./Feb. 1994.

[4] J. Kim and S. Sul, "New approach for high-performance PMSM drives without rotational position sensors," *IEEE Trans. Power Electron.*, vol. 12, pp. 904–911, Sept. 1997.

[5] S. Bolognani, R. Oboe, and M. Zigliotto, "Sensorless full-digital PMSM drive with EKF estimation of speed and rotor position," *IEEE Trans. Ind. Electron.*, vol. 46, pp. 184–191, Feb. 1999.

[6] R. Dhaouadi, N. Mohan, and L. Norum, "Design and implementation of an extended Kalman filter for the state estimation of a permanent magnet synchronous motor," *IEEE Trans. Power Electron.*, vol. 6, pp. 491–497, July 1991.

[7] M. Tomita, T. Senjyu, S. Doki, and S. Okuma, "New sensorless control for brushless DC motors using disturbance observers and adaptive velocity estimations," *IEEE Trans. Ind. Electron.*, vol. 45, pp. 274–282, Apr. 1998.

[8] T. Orlowska-Kowalska, "Comparison of speed estimation methods for the sensorless permanent magnet AC drives," in *Proc. Power Electronics and Motion Control Conf. (PEMC'98)*, Prague, Czech Republic, Sept. 1998, pp. 5.266–5.271.

[9] J. Solsona, M. I. Valla, and C. Muravchik, "A nonlinear reduced order observer for permanent magnet synchronous motors," *IEEE Trans. Ind. Electron.*, vol. 43, pp. 492–497, Aug. 1996.

[10] J. A. Solsona, M. I. Valla, and C. H. Muravchik, "Comparison of a linear and a nonlinear observer for rotor position and speed estimation in permanent magnet AC drives," *Latin Amer. Appl. Res.*, vol. 29, no. 3/4, pp. 197–203, 1999.